Biomedicine & Pharmacotherapy 158 (2023) 114083

Contents lists available at ScienceDirect

Biomedicine & Pharmacotherapy

journal homepage: www.elsevier.com/locate/biopha

A potential host and virus targeting tool against COVID-19: Chemical characterization, antiviral, cytoprotective, antioxidant, respiratory smooth muscle relaxant effects of *Paulownia tomentosa* Steud

Fabio Magurano [a,*,1], Matteo Micucci [b,1], Domenico Nuzzo [c], Melissa Baggieri [a], Pasquale Picone [c], Silvia Gioacchini [a], Raoul Fioravanti [a], Paola Bucci [a], Maedeh Kojouri [a], Michele Mari [b], Michele Retini [b], Roberta Budriesi [d], Laura Beatrice Mattioli [d], Ivan Corazza [e], Valentina Di Liberto [f], Luigi Todaro [g], Roberto Giuseppetti [a], Emilio D'Ugo [a], Antonella Marchi [a], Marisabel Mecca [h], Maurizio D'Auria [h]

[a] *Department of Infectious Diseases, Istituto Superiore di Sanità (ISS), Rome, Italy*
[b] *Department of Biomolecular Sciences, University of Urbino Carlo Bo, Piazza Rinascimento 6, 61029 Urbino, PU, Italy*
[c] *Istituto per la Ricerca e l'Innovazione Biomedica, CNR, via U. La Malfa 153, 90146 Palermo, Italy*
[d] *Department of Pharmacy and Biotechnology, Food Chemistry and Nutraceutical Lab, Alma Mater Studiorum-University of Bologna, 40126 Bologna, Italy*
[e] *Department of Specialistic, Diagnostic and Experimental Medicine (DIMES), University of Bologna, S. Orsola-Malpighi University Hospital, Alma Mater Studiorum-University of Bologna, Bologna, Italy*
[f] *Department of Biomedicine, Neuroscience and Advanced Diagnostic, University of Palermo, 90128 Palermo, Italy*
[g] *Scuola di Scienze Agrarie, Forestali, Alimentari ed Ambientali, Università della Basilicata, Via dell'Ateneo Lucano 10, 85100 Potenza, Italy*
[h] *Dipartimento di Scienze, Università della Basilicata, Via dell'Ateneo Lucano 10, 85100 Potenza, Italy*

ARTICLE INFO

Keywords:
COVID-19
Paulownia tomentosa Steud extract
Antiviral
Antioxydant
Phytocomplex
SARS-CoV-2

ABSTRACT

COronaVIrus Disease 2019 (COVID-19) is a newly emerging infectious disease that spread across the world, caused by the novel coronavirus Severe Acute Respiratory Syndrome CoronaVirus 2 (SARS-CoV-2). Despite the advancements in science that led to the creation of the vaccine, there is still an urgent need for new antiviral drugs effective against SARS-CoV-2. This study aimed to investigate the antiviral effect of *Paulownia tomentosa* Steud extract against SARS-CoV-2 and to evaluate its antioxidant properties, including respiratory smooth muscle relaxant effects. Our results showed that *P. tomentosa* extract can inhibit viral replication by directly interacting with both the 3-chymotrypsin-like protease and spike protein. In addition, the phyto complex does not reduce lung epithelial cell viability and exerts a protective action in those cells damaged by tert-butyl hydroperoxide , a toxic agent able to alter cells' functions via increased oxidative stress. These data suggest the potential role of *P. tomentosa* extract in COVID-19 treatment, since this extract is able to act both as an antiviral and a cyto-protective agent in vitro.

1. Introduction

The COronaVIrus Disease 2019 (COVID-19) pandemic has been caused by the enveloped Betacoronavirus Severe Acute Respiratory Syndrome CoronaVirus 2 (SARS-CoV-2), transmitted from person to person through respiratory droplets and direct contact, and potentially by indirect contact through fomites [1].

The clinical spectrum of COVID-19 ranges from asymptomatic or paucisymptomatic forms to clinical pathologies characterized by a wide spectrum of symptoms involving severe conditions such as acute respiratory failure requiring mechanical ventilation, septic shock, and multiple organ failure [2–6].

The disease resulted in high occurrences of fatal pneumonia with clinical symptoms resembling those of severe acute respiratory syndrome (SARS), a viral respiratory illness caused by the SARS-associated coronavirus (SARS-CoV), during the 2002–2004 SARS epidemic.

* Corresponding author.
E-mail address: fabio.magurano@iss.it (F. Magurano).
[1] These authors equally contribute to the work

https://doi.org/10.1016/j.biopha.2022.114083
Received 14 September 2022; Received in revised form 23 November 2022; Accepted 2 December 2022
Available online 5 December 2022

Symptoms included persistent fever, chills/rigor, myalgia, malaise, dry cough, headache and dyspnoea [7].

Since its appearance, up to the end of October 2022 over 615 million cases have been reported worldwide, including over 6 million deaths [8].

Epidemiological studies suggest that COVID-19 severity overall correlates with several comorbidities, including diabetes, obesity, cardiovascular diseases, and immunosuppressive conditions. Patients with such comorbidities exhibit elevated levels of reactive oxygen species (ROS) and oxidative stress caused by an increased accumulation of angiotensin II and by the activation of the Nicotinamide Adenine Dinucleotide PHosphate (NADPH) oxidase pathway. Moreover, evidences suggest that oxidative stress coupled with the cytokine storm contributes to COVID-19 pathogenesis and immunopathogenesis causes endotheliitis and endothelial cell dysfunction and activates the blood clotting cascade that results in blood coagulation and microvascular thrombosis [9,10].

According to the World Health Organization (WHO), about 80% of the world's population relies on medicinal plants or herbs to fulfil their medical needs [11]. Natural compounds with many biological activities involving antiviral, antioxidant, anti-inflammatory and respiratory smooth muscle relaxing properties were investigated in an attempt to contribute to global research for discovering effective therapeutic agents in the treatment of coronavirus infections and their clinical complications. Also concerning COVID-19, the identification of integrative therapies or new antiviral therapies is still important. In this context, the investigation of compounds from terrestrial and marine plants may also lead to the discovery of new bioactive molecules [12–14].

Based on the literature, antioxidant substances may offer a potential integrative option. Some plant secondary metabolites, including flavonoids and limonoids, exhibit both antiviral action in models of coronavirus infections and antioxidant effects [15,16]. Several flavonoids, in addition to inhibiting SARS-CoV-2 in vitro, exert a plethora of biological activities resulting in cardiovascular system protection [17,18]. For some flavonoids, the antiviral activity has been mainly attributed to the inhibition of the 3-chymotrypsin-like protease ($3CL^{pro}$) of SARS-CoV-2, as this enzyme plays a major role during viral replication [19]. Also, clinical data suggest the efficacy of vegetal extracts rich in polyphenols as a coadjuvant in the treatment of COVID-19 [20].

Several compounds extracted from plant matrices, in addition to antioxidant and mildly anti-inflammatory activities, have antimicrobial effects against different viruses, including coronaviruses. It is the case of glycyrrhizin, withaferin A, curcumin, nigellidine and cordifolioside A, able to inhibit SARS-CoV-2 replication and reduce host inflammation response [21]. Similar observations may be reported for phyto complexes [22,23]. The observation that the same substance is capable to inhibit viral replication and reducing the molecular phenomena, triggered by the infection that produces the inflammatory state, constitutes an element of novelty. This spectrum of activity could be explained by a multi-components-multitarget paradigm on the effects of different phyto complexes and compounds isolated from the plant kingdom. These data provided support to the investigation of phyto complexes and isolated compounds as potential nutraceutical approaches in the management of COVID-19 disease and its severe clinical complications, including long-COVID-related symptoms [24].

In this paper, we present a study on an extract from waste wood of *Paulownia tomentosa* Steud . This plant, with a long history of use for medical purposes in China belongs to the family of Paulowniaceae, and represents a rich source of biologically active secondary metabolites, such as flavonoids, lignans, phenolic glycosides, quinones, terpenoids, glycerides, phenolic acids, and other compounds [25,26].

Several geranylated flavonoids isolated from this plant were shown to inhibit SARS-CoV papain-like protease [27], suggesting its antiviral activity against SARS-CoV-2 in vitro.

P. tomentosa extract was obtained by the treatment of wood wastes in an autoclave, in the presence of micrometric crystals of H3PMo12O40, according to the method previously described [28].

The aim of our study was to investigate the biological effects of *P. tomentosa* extract, including antiviral effects against SARS-CoV-2, antioxidant and respiratory smooth muscle modulation properties, using in vitro experimental models, that may result in clinical benefits in COVID-19 patients.

The results obtained represent the basis for a further investigation aimed at clinical applications of this phyto complex in COVID-19 and may lead to the development of medical devices.

2. Methods

2.1. Sample preparation and treatment

In this work, wooden boards of *P. tomentosa* (0.5 m 3; dimensions: 30 × 180 × 1500 mm) without defects, supplied by the local manufacturers, were used as raw materials. Boards were thermally modified with a vacuum plant, developed by WDE Maspell srl (Terni, Italy), located at the University of Basilicata. This method consists in placing the boards between two metal plates, which contain diathermic hot oil that provides conductive heat transfer to the boards. Pressure in the kiln can be regulated in the range of 60–1000 mbar. The vacuum is maintained through a water ring-type pump equipped with a heat exchanger. Under pressure, the plates provide a force on the boards that prevents potential deformation of the wood [29]. Drying and thermal treatment were applied in the same plant.

The thermal modification started after drying by gradually increasing the temperature to 210 °C (maintained for 3 h). Total treatment including the cooling phase lasted 15 h. More details regarding the Thermo-Vacuum process and its technical particularities were previously described [29,30].

The mass loss, due to the thermal treatment, was determined by weighting each treated board immediately after the drying process (when the wood moisture content was 0%) and at the end of the thermal treatment.

2.2. Chemical characterization

Treated and untreated wood samples were randomly selected and reduced to a small size with a mill saw and subjected to Soxhlet extraction technique with 1:2 ethanol-toluene mixture for 7 h in a Soxhlet apparatus by using the TAPPI test method T204 [31]; 1 g of milled wood repeated three times was used.

The extraction apparatus consisted of a 500 ml flask, Soxhlet tube, and 300-mm Allihn condenser.

Samples were put in cellulose thimbles (33 × 80 mm) of medium porosity. After the extraction, the solution was dried in a previously weighed 25 ml flask, by using a rotary evaporator connected to a vacuum pump (Vacuumbrand PC3001). The percentage of extractives were determined gravimetrically by weighing the flask containing the residue and comparing the weight to that of the initial dry mass wood.

The obtained mixture was fractionated as follows: the mixture was treated with chloroform (20 ml) and filtered. The solvent was evaporated, and the residue was chromatographed by using tin layer chromatography. The eluent was 1:1 hexane-ethyl acetate. Qualitative and quantitative measurements of the extracts were then made by the analytical method using a Gas Chromatography–Mass Spectrometry (GC-MS) system. GC-MS analyses were performed on an HP 6890 (Agilent) GC system equipped with an HP 5963 MS selective detector, with a high-temperature capillary column (HP-5MS, 30 m × 0.25 mm I. D., 0.25-μm film thickness; J& W Scientific, CA, USA) and helium as carrier gas. Samples were injected directly into the column at the temperature of 80 °C. After injection, the temperature was held at 80 °C for 3 min, and then heated to 250 °C at a rate of 20 °C min − 1 and held for 20 min. Compounds were identified by computer comparison of the mass spectra with NIST libraries and by mass fragmentation patterns.

The lignin content was determined as follows. The sawdust was transferred to a 50 ml beaker, a cold H_2SO_4 solution (72%, 15 ml) was added, and the mixture was frequently stirred for 2 h at room temperature. The mixture was then diluted to 3% (w/w) with 560 ml of distilled water, heated under reflux for 4 h, filtered, and washed with 500 ml of water. The residue was dried at 105 °C to a constant mass. The holocellulose content was determined by the difference between the amount of residue after extraction and the lignin content.

2.3. Cell cultures and treatment

Lung epithelial cell line H292 (ATCC NCI-H292 [H292] CRL-1848) were cultured with Roswell Park Memorial Institute (RPMI) 1640 medium and supplemented with 10% fetal bovine serum (FBS), 100 U/ml penicillin and 100 U/ml streptomycin (Sigma) and 2 mM L-glutamine in a humidified atmosphere of 95% air and 5% CO_2 at 37 °C. In cell viability time-course and dose-effect experiments the cells received the following treatment: 0.01, 0.1 and 1 mg/ml of *P. tomentosa* extract for 24 and 48 h. In Tert-Butyl Hydroperoxide (TBH, Luperox® TBH70X, Merck Life Science S.r.l., Italy) cell viability dose-effect experiments, TBH 50, 100 and 150 μM for 24 h; in protection experiments against TBH-induced toxicity and oxidative stress, TBH 150 μM for 24 h, *P. tomentosa* extract (0.1 mg/ml) +TBH (150 μM) for 24 h (co-treatment), *P. tomentosa* extract (0.1 mg/ml) for 24 h. The no-treatment control (Ctrl) received an equal volume of the medium.

Vero E6 (Cercopithecus aethiops derived epithelial kidney, C1008 ATCC CRL-1586) cells were grown in Minimum Essential Medium (MEM + GlutaMAX, Gibco) supplemented with 10% Fetal Calf Serum (FCS), 100 U/ml penicillin, 100 U/ml streptomycin, 1 mM sodium pyruvate, and 1% non-essential amino acids.

2.4. Cell viability and morphology

H292 cells were grown at a density of 2×10^4 cells/well on 96-well plates in a final volume of 100 μL/well. After the treatment, cell viability was assessed by 3-(4,5-dimethylthiazol-2-yl)− 2,5-diphenyltetrazolium bromide (MTT, Sigma-Aldrich) assay, as previously described [32]. After 2 h of incubation, after dissolving formazan crystals with dimethyl sulfoxide (DMSO) 100 μL/well, absorbance was measured at 570 nm with background subtraction. Cell viability was expressed as arbitrary units, with Ctrl set to 1. For the analysis of cell morphology, the cellular images were obtained using the Zeiss Axio Scope 2 microscope (Carl Zeiss, Oberkochen, Germany).

Vero E6 cells were grown at a density of 1×10^4 cell/well in 96-well plates and treated for 24 h with *P. tomentosa* extract (from 1 mg/ml to 0.01 mg/ml). Then, a XTT assay (Cell Proliferation Kit II, Roche) was performed as previously described [15]. The measured absorbance directly correlates with the number of viable cells.

2.5. Antioxidant effect against Reactive Oxygen Species (ROS)

In the measurement of ROS generation, H292 cells were plated at a density of 1×10^4 cells/well on 96-well plates in a final volume of 100 μL/well. TBH at 150 μM was used to induce the oxidative stress, alone or in combination whit 0.01 and 0.1 mg/ml of *P. tomentosa* extract. At the end of the treatments, dichlorofluorescein diacetate (DCFH-DA) was added to each sample at the final concentration of 1 mM (Invitrogen, Monza, Italy) and incubated for 30 min in the dark at 37 °C. After washing with PBS, the cells were analyzed by measuring the fluorescence intensity with a Microplate Reader GloMax fluorimeter (Promega Corporation, Madison, WI 53711 USA) at Ex/Em: ~492–495/517–527 nm. In addition, the cells were analyzed by a fluorescence microscope (Axio Scope 2 microscope; Zeiss, Oberkochen, Germany).

2.6. Virus propagation

Viral isolate BetaCov/Italy/CDG1/2020|EPI ISL 412973|2020–02–20 (GISAID accession ID: EPI_ISL_412973), was propagated as previously described [33]. Virus propagation was conducted within biosafety-level-3 facilities at Istituto Superiore di Sanità (Rome, Italy).

2.7. Plaque reduction neutralization test

Plaque Reduction Neutralization Test (PRNT) assay was used to assess the virucidal potential of *P. tomentosa* extract against SARS-CoV-2. The natural compound was resuspended in 30% DMSO, to a final concentration of 1 mg/ml that did not affect the growth of the cells in vitro. Then, serial dilutions of the extract (from 0.1 to 0.001 mg/ml) were incubated with 80 PFU of SARS-CoV-2 at 4 °C overnight (~16 h). The mixtures were added in triplicates to confluent monolayers of Vero E6 cells, grown in 12-well plates and incubated at 37 °C in a humidified 5% CO_2 atmosphere for 60 min. Then, 4 ml/well of a medium containing 2% Gum Tragacanth + MEM 2X supplemented with 2.5% of heat-inactivated FCS was added. Plates were left at 37 °C with 5% CO_2. After 3 days, the overlay was removed, and the cell monolayers were washed with PBS to completely remove the overlay medium. Cells were stained with a crystal violet 1.5% alcoholic solution. The presence of SARS-CoV-2 virus-infected cells was indicated by the formation of plaques. The half-maximal inhibitory concentration (IC_{50}) was determined as the highest dilution of the substance resulting in a 50% ($PRNT_{50}$) reduction of plaques as compared to the virus control and it was calculated using GraphPad Prism software.

2.8. Antiviral activity

Vero E6 cells were seeded in 24-well plates at a concentration of 200 000 cells/well. After 24 h of incubation at 37 °C, plates were infected with SARS-CoV-2 at 0.01 multeplicity of infection (MOI) and incubated 1 h at 37 °C. Then, 2 ml of *P. tomentosa* extract, diluted at the concentration of 0.1 mg/ml in medium, was added to each infected well in triplicate. Plates were left at 37 °C in a humidified 5% CO_2 atmosphere. After 24 h, the cytopathic effect was observed, and each culture supernatant was collected for RNA extraction and virus titration for viral quantification. The 50% Tissue Culture Infectious Dose ($TCID_{50}$) assay was performed on the harvested samples as previously described [33], and the RNAs extracted were tested by Real-time PCR to target the N gene of SARS-CoV-2 based on protocols developed by the Centers for Disease Control and Prevention [34].

2.9. Surface Plasmon Resonance

Binding studies were performed through Surface Plasmon Resonance (SPR) on Biacore X100 (Cytiva). $3CL^{pro}$ (ProteoGenix, Schiltigheim, France) and SARS-CoV-2 (S) protein (Acc. # YP_009724390.1; R&D Systems, Minneapolis, USA) were immobilized on a CM5 sensor chip by the amine coupling method as per manufacturer instructions by using Acetate pH 5.0 and pH 4.0 respectively and final protein concentration of 50 μg ml^{-1} [35,36]. PBS-P + (10 mM phosphate buffer, 150 mM NaCl, 0.05% surfactant P20) supplemented with 5% DMSO was used as running and dilution buffer per manufacturer instructions. Serial dilutions of analyte were injected at 25 °C with a flow rate of 30 μL min^{-1}. The surface was regenerated between samples with a 70% ethylene glycol solution per manufacturer instructions. All data were zero adjusted and the reference (blank) was subtracted. The quality of the fitted results was evaluated by the χ^2 parameter.

2.10. In vitro functional studies

2.10.1. Animals

Guinea-pig of either sex (200–400 g) obtained from Charles River

(Calco, Como, Italy) were used. The animals were housed according to the ECC Council Directive regarding the protection of animals used for experimental and other scientific purposes. All procedures followed the guidelines of the animal care and use committee of the University of Bologna (Protocol PR 21.79.14). The animals were sacrificed by cervical dislocation. The trachea and lungs were set up rapidly under a suitable resting tension in 15 ml of an organ bath containing appropriate physiological salt solution consistently warmed (see below) and buffered to pH 7.4 by saturation with 95% O_2 - 5% CO_2 gas.

2.10.2. Guinea-pig trachea

The method described by Budriesi et al. [37] was modified as described above. The trachea was cut transversally between the segment of cartilage and four groups of the tracheal segments, each one made up of three rings, were tied together and mounted under a tension of 1 g at 37 °C in an organ bath containing Krebs-Ringer solution of the following composition (mM): NaCl 95, KCl 4.7, $CaCl_2$ 2.50, $MgSO_4$ 1.0, KH_2PO_4 1.17, $NaHCO_3$ 25, and glucose 10.6, equilibrated with 95% O_2-5% CO_2 gas at pH 7.4. Tissues were allowed to stabilize for 90 min. The tension was recorded isometrically. The rings were allowed to stabilize for 60 min. A constant tone level was induced by Carbachol (CCh) chloride (0.5 μM), and after 15 min, a cumulative concentration-response curve to isoprenaline, extracts, magnolol and honokiol was done. All responses to different concentrations of compounds and extracts were expressed as a percentage of the maximal relaxation recorded isometrically. Data of ß-receptor agonism is presented as mean ± S.E.M. The IC_{50} were calculated from concentration-response curves and were analyzed by the Student's t-test and presented as means ± S.E.M.

2.10.3. Guinea-pig lung

The procedure was previously described [38]. Briefly, strips of peripheral lung tissue, approximately 15 × 2 x 2 mm, were cut either from the body of a lower lobe with the longitudinal axis of the strip parallel to the bronchus or from the peripheral margin of the lobe and set up under 0.3 g tension at 37 C in organ baths containing Krebs-Henseleit buffer solution (composition (mM): NaCl 118.78, KCI 4.32, $CaCl_2$ 2.52, $MgSO_4$ 1.18, KH_2PO_4 1.28, $NaHCO_3$ 25 and glucose 5.5). Tension changes were recorded isometrically.

2.10.4. Trachea ring and lung spontaneous contractility

The experimental design was previously described [39]. Briefly, for the trachea and lung the tracing graphs of spontaneous contractions were continuously recorded with the LabChart Software (ADInstruments, Bella Vista, New South Wales, Australia). After the equilibration period (about 30–45 min according to each tissue) cumulative concentration curves of extracts and reference compounds were constructed. At the end of every single dose, the following parameters of the Spontaneous Contraction (SC) recording were evaluated considering a 5 min stationary period: the Mean Spontaneous Contraction Amplitude (MCA), evaluated as the mean force value (g); the standard deviations of the force values over the period, as an index of the Spontaneous Contraction Variability (SCV); and Basal Spontaneous Motor Activity (BSMA), as the percentage (%) variation of each mean force value (g) with respect to the control period. The SCs were investigated in the frequency domain through a standard FFT analysis and a subsequent Power Spectral Density (PSD) plot. The absolute powers of the following frequency bands of interest—low [0.0,0.2[Hz (LF), medium [0.2,0.6[Hz (MF) and high [0.6,1.0] Hz (HF) [40] were then calculated. The PSD percentage (%) variations for each band of interest with respect to control were estimated.

2.10.5. β-agonist activity

The trachea was prepared as previously described [37], using the PSS described above. The rings were allowed to stabilize for 60 min. A constant tone level was induced by CCh chloride (0.5 μM), and after 15 min, a cumulative concentration-response curve to isoprenaline, extracts, magnolol and honokiol was done. All responses to different concentrations of compounds and extracts were expressed as a percentage of the maximal relaxation recorded isometrically. Data of ß-receptor agonism are presented as mean ± S.E.M. The IC_{50} were calculated from concentration-response curves and were analyzed by the Student's t-test and presented as means ± S.E.M.

2.11. Statistical analysis

Data analysis was performed using GraphPad Prism 8.4.3 software (GraphPad Software, Inc, La Jolla, CA, USA). The results are presented as mean ± SE, and expressed as arbitrary units, with controls equal to 1. Statistical evaluations were performed by one-way ANOVA, followed by Tukey Post-Hoc test. Differences in a p-value less than 0.05 were considered statistically significant.

The IC_{50} value from the PRNT assay was calculated using GraphPad Prism version 9.0.0 (GraphPad Software, LLC., San Diego, USA) for Windows. The potency of extracts defined as IC_{50} were calculated from concentration-response curves Probit analysis using Litchfield and Wilcoxon [41] and GraphPad Prism® software [42,43].

3. Results

3.1. Chemical characterization

The thermo-treated wood showed the following composition: the extractives represented 10.2% (w/w) of the wood, lignin was 39.5%, while holocellulose represents 50.3% of the weight of wood.

A major part of extractives is soluble in chloroform (87.2%). Table 1 collects the compounds found in the GC-MS analysis of chloroform soluble fraction of the extractives.

3.2. Effects of P. tomentosa extract on H292 cell viability

A dose-effect study on cell viability was performed by MTT assay on lung epithelial cell H292, treated with *P. tomentosa* extract for 24 h. For this analysis, we investigated three different *P. tomentosa* extract doses: 0.01 mg/ml, 0.1 mg/ml and 1 mg/ml. The results in Fig. 1 show that 0.01 mg/ml and 0.1 mg/ml *P. tomentosa* extract treatment did not induce any significant change in cell viability (Fig. 1 A, C). Conversely, cell viability significantly decreased after 1 mg/ml *P. tomentosa* extract exposure (Fig. 1 B). When the treatment with *P. tomentosa* extract was

Table 1
GC-MS analysis of the chloroform soluble fraction of *P. tomentosa* extractives. Total phenolic content was determined as 750 mg gallic acid equivalent (GAE)/g, while total flavonoid content was 1800 mg quercetin equivalent (QE)/g.

Compound	R.T. [min.]
Piperonal	8.26
2,6-Dimethoxyphenol	8.30
5-(1-propenyl)− 1,3-benzodioxole	8.47
1-(3,4-methylenedioxy) phenyl-1,2-propanedione	9.57
4-hydroxy-3,5-dimethoxybenzaldehyde	10.31
3-(4-hydroxy-3-methoxy)− 2-propenal	10.82
Heptadecene	10.84
Methyl hexadecanoate	11.52
Methyl 14-methylpentadecanoid acid	11.55
Hexadecanoic acid	11.74
3,5-dimethoxy-4-hydroxycinnamaldehyde	12.11
Methyl 8-octadecenoate	12.54
1,13-Tetradecadiene	12.64
Methyl stearate	12.70
Octadecanoic acid	12.94
Butyl citrate	13.70
Pentacosane	13.97
Eicosane	16.19
Sesamin	16.28
Episesamin	17.15

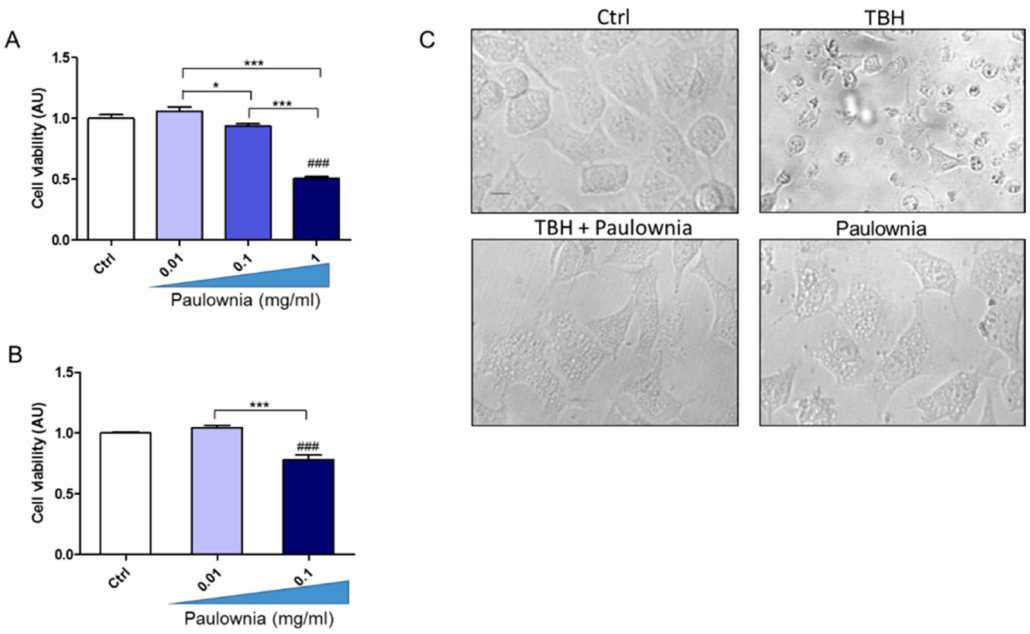

Fig. 1. Effects of *P. tomentosa* extract (Paulownia) treatments on cell viability of H292 cells for 24 and 48 h. A) Histogram of MTT cell viability assay for 24 h. B) Histogram of MTT cell viability assay for 48 h. C) Representative morphological images of untreated cells (Ctrl) and treated with 0.1 mg/ml of the *P. tomentosa* extract (Paulownia). Bar: 50 μm. Tukey test: ## $p < 0.01$, ### $p < 0.001$ as compared to Ctrl group; * $p < 0.05$, * ** $p < 0.001$.

prolonged up to 48 h, a slight but significant decrease in cell viability was associated with the 0.1 mg/ml dose.

3.3. Effects of P. tomentosa extract on cell viability impaired by TBH treatment

We analyzed oxidative agent TBH sensitivity using MTT and DCHF-DA assays on H292 lung epithelial cells [44]. As the dose-effect shown in Fig. 2, H292 cells treated with TBH at 100 μM induce a 60% reduction in cell viability (Fig. 2 A). Based on these results we choose a concentration of 150 μM for the subsequent experiments. *P. tomentosa* extract was able to protect the H292 cell under stress conditions; when treated with TBH 150 μM in combination with increasing concentrations of *P. tomentosa* extract after 24 and 48 h. As detected by the MTT assay, the extract was able to inhibit the toxicity induced by TBH in a dose-dependent manner, reaching a viability value comparable to the control at the concentration of 0.1 mg/ml of *P. tomentosa* extract after 24 h of treatment (Fig. 2B). The long stimulation with TBH for 48 h is not able to revert the cell damage (Fig. 2 C).

3.4. Effects P. tomentosa extract on ROS generation by TBH treatment

The ability of *P. tomentosa* extract to decrease ROS production induced by TBH treatment was analyzed by DCFH-DA assay. The result was evaluated by fluorescence microscopy observation (Fig. 2D) and fluorimeter analysis (Fig. 2E), in which control cells (untreated) or treated cells with *P. tomentosa* extract at different doses, did not show any fluorescence, indicating that the extract did not induce oxidative stress. In contrast, the treatment with *P. tomentosa* extract abolished the TBH-induced ROS production (Fig. 2 D, E).

3.5. Virucidal Activity on SARS-CoV-2

Concentrations of *P. tomentosa* extract from 0.1 to 0.001 mg/ml were chosen to test virucidal activity in Vero E6 monolayers. Cell viability XTT analysis was not affected by the extract up to the concentration of 1 mg/ml (Fig. 3 A). The virucidal activity against SARS-CoV-2 was evaluated in vitro through $PRNT_{50}$, tested in triplicates, and a concentration required to inhibit 50% of infection was used as the cut-off threshold of virucidal activity. The results demonstrated that *P. tomentosa* extract was effective against SARS-CoV-2, with an IC_{50} value of 0.0035 mg/ml, calculated using GraphPad Prism (V. 9.0.0), as shown in Fig. 3B.

3.6. Antiviral Activity

The antiviral activity against SARS-CoV-2 was measured by comparing infection levels in *P. tomentosa* extract -treated and untreated Vero E6 cultures. The 0.1 mg/ml concentration (that did not affect the growth of Vero E6 monolayers and showed a significant virucidal effect in our previous experiments) was chosen to investigate SARS-CoV-2 replication inhibition and the antiviral activity of this compound. The antiviral effects of *P. tomentosa* extract were evaluated using $TCID_{50}$ assay in Vero E6 cells, to quantify the virus titer in the supernatants from infected cells in which the *P. tomentosa* extract was added.

The quantification of the antiviral activity was also evaluated by Real-Time RT-PCR in terms of Ct threshold of the amplification of the N gene of the virus.

The results show a remarkable antiviral effect on the infected cells at 24 h post-infection (hpi) as shown in Fig. 3D, E.

3.7. Results of SPR

The *P. tomentosa* extract was utilized in SPR measurements to investigate the interaction of its components with two major structural and non-structural proteins hallmarks of SARS-CoV-2 host recognition/insertion and viral replication, i.e. the S protein and the $3CL^{pro}$ (also known as Main Protease Mpro), to explain its antiviral activity seen in in vitro studies. Given the complexity of the sample, the affinity evaluation was not possible due to the unknown concentration of the active compounds and the diversity of molecular weights. Qualitative analysis of the sensorgrams clearly shows that the extract interacts efficiently with $3CL^{pro}$ as well as with S protein (Fig. 4). The strength of the protein-inhibitor complex is clearly visible from the rate of the signal decay during the stability phase ($t > 45$ s) which is quite slow in comparison with common small molecules between 400 and 200 Da, for which the

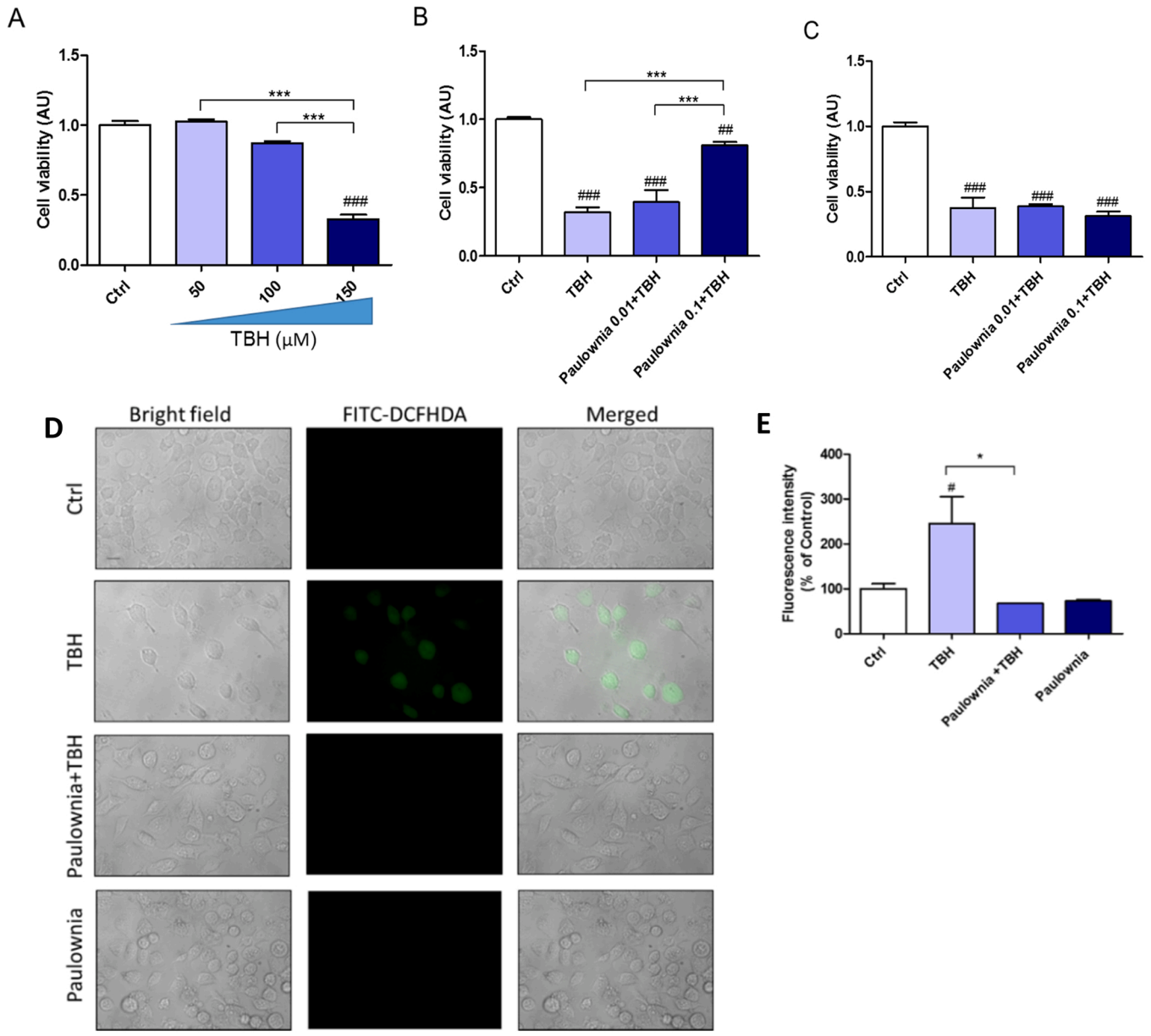

Fig. 2. Oxidative insult and effects of *P. tomentosa* extract (Paulownia) treatment on ROS production in H292 cells. A) Dose-effect of TBH treatment (24 h) on cell viability. B) Cytoprotective effect of *P. tomentosa* extract treatment (24 h) on cells treated with TBH (24 h, 150 μM). C) Cytoprotective effect of *P. tomentosa* extract treatment (48 h) on cells treated with TBH (24 h, 150 μM). D) Bright field, Fluorescence microscopy (FITC-DCFHDA) and merged images of untreated cells (Ctrl) and cells treated with TBH, or *P. tomentosa* extract or a combination of *P. tomentosa* extract and TBH for 24 h. E) FITC-DCFHDA fluorescence intensity quantification. Bar: 50 μm. Tukey test: # $p < 0.05$ as compared to Ctrl group; * $p < 0.05$.

complete dissociation of the complex (the signal returns to the baseline value) is usually observed within 30–40 s. From the association phase is possible to deduce the stoichiometry of the interaction, which probably involves more than a single compound since the sensorgram presents discontinuities that suggest the participation of fast interactions added to another slower ones.

3.8. Effects of P. tomentosa extract on airways contractility

The *P. tomentosa* extract was studied on trachea and lung spontaneous contractility and cumulative concentration-response curves were realized.

The phyto complex, in the trachea, decreases tone up to the concentration of 0.5 mg/ml (Fig. 5). At the same concentration, low-frequency waves undergo a significant increase.

In the lungs, the extract determines smooth muscle relaxation in a concentration-dependent manner, up to a maximum percentage of 16% (Fig. 5). In this tissue, *P. tomentosa* extract increases low-frequency waves up to a stable value.

4. Discussion

After more than two years into the pandemic, with over one million new infections and thousands of deaths around the world every day, COVID-19 continues to strain healthcare systems and exact a terrible human toll. Despite vaccines remaining the most important way to rein in the pandemic, there is still a desperate need for better therapies to treat people who cannot access vaccines, and whose immune systems cannot respond fully to vaccination, or who experience breakthrough infections. Moreover, new medications can intervene whenever vaccines

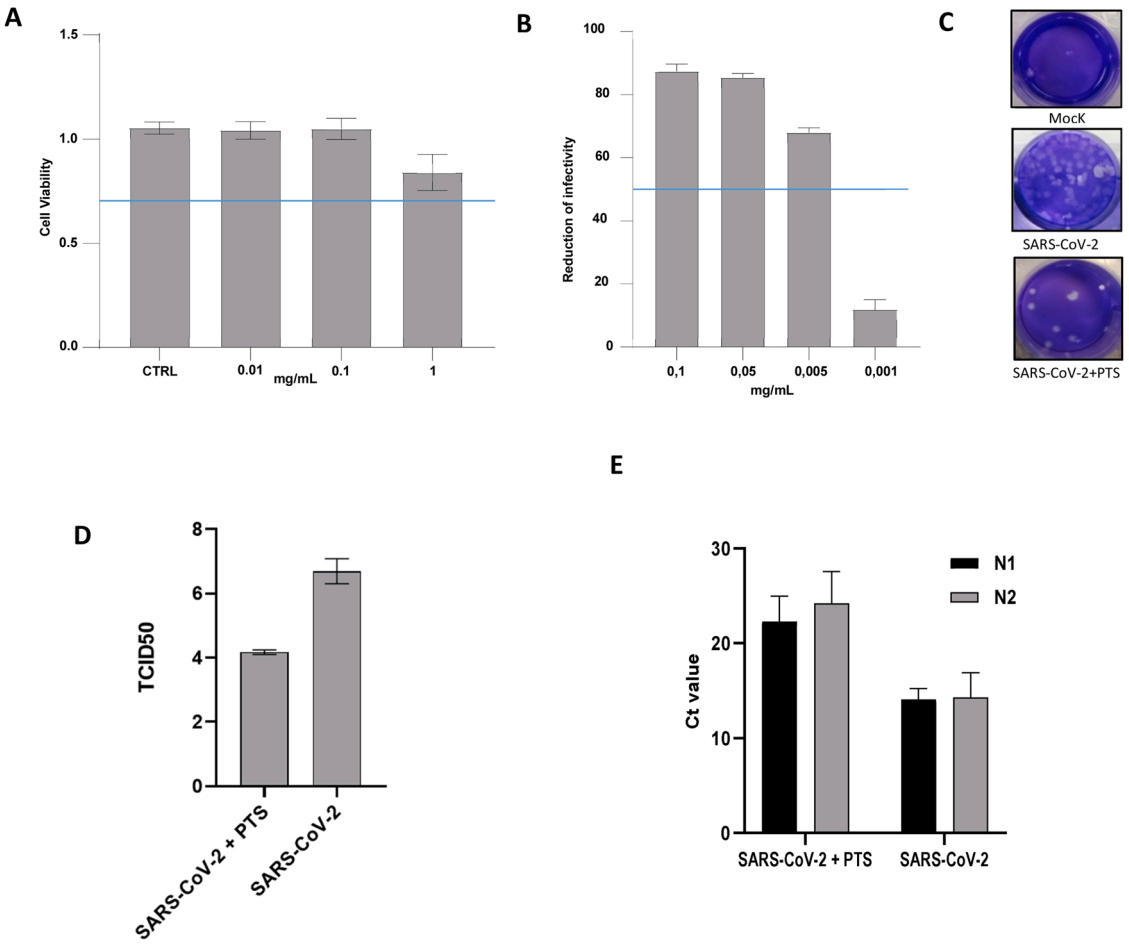

Fig. 3. A) Results of XTT assay on cells incubated with different concentrations of *P. tomentosa* extract (from 1 to 0.01 mg/ml). Cell viability was not affected by the *P. tomentosa* extract at the concentrations tested. B) Results of PRNT assay on serial dilutions of *P. tomentosa* extract (from 0.1 to 0.001 mg/ml) to assess the virucidal activity against SARS-CoV-2: *P. tomentosa* extract was effective against SARS-CoV-2 until the concentration of 0.005 mg/ml with an Ic_{50} value of 0.0035 mg/ml. C) SARS-CoV-2 plaques after fixing and staining with crystal violet at 72 hpi. D) Results of $TCID_{50}$ assay performed on Vero E6 cells treated with *P. tomentosa* (PTS) extract at the concentration of 0.1 mg/ml and untreated cultures, infected at 0.01 MOI: there is an evident decrease in viral titer comparing infected cells treated with PTS and untreated ones. E) Results of Real-time RT-PCR by Ct values of SARS-CoV-2 N1 and N2 gene targets (mean of triplicates) on supernatants of cells treated at 0.1 mg/ml and untreated , harvested at 24 hpi: the same results are confirmed even by the reduction of the viral genome when supernatants are treated with PTS.

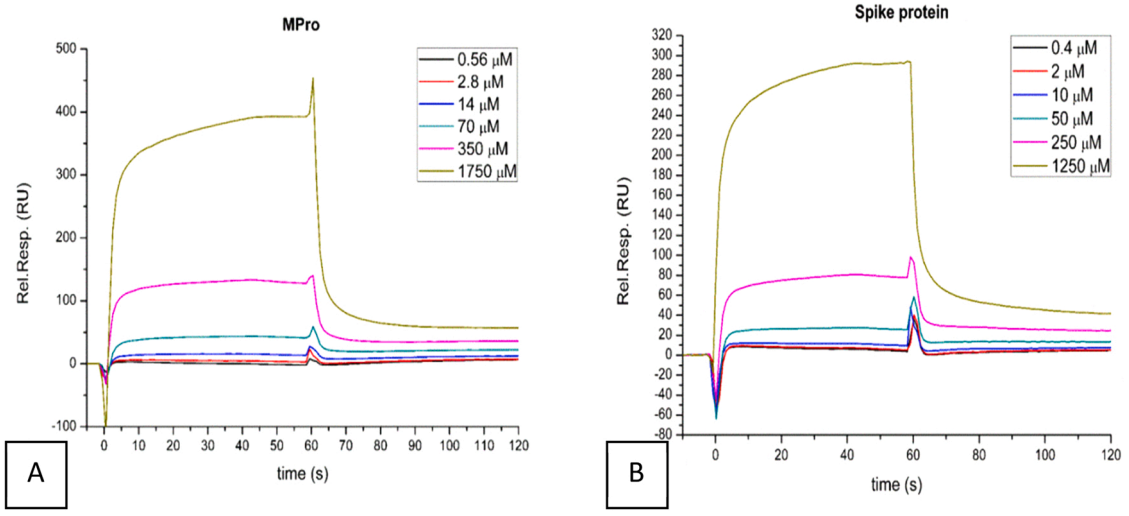

Fig. 4. Results from SPR: sensorgrams show that *P. tomentosa* extract interacts efficiently with M^{pro} (A) as well as with Spike protein (B). The strength of the protein-inhibitor complex can be inferred from the rate of the signal decay during the stability phase ($t > 45$ s) which is quite slow in comparison with common small molecules.

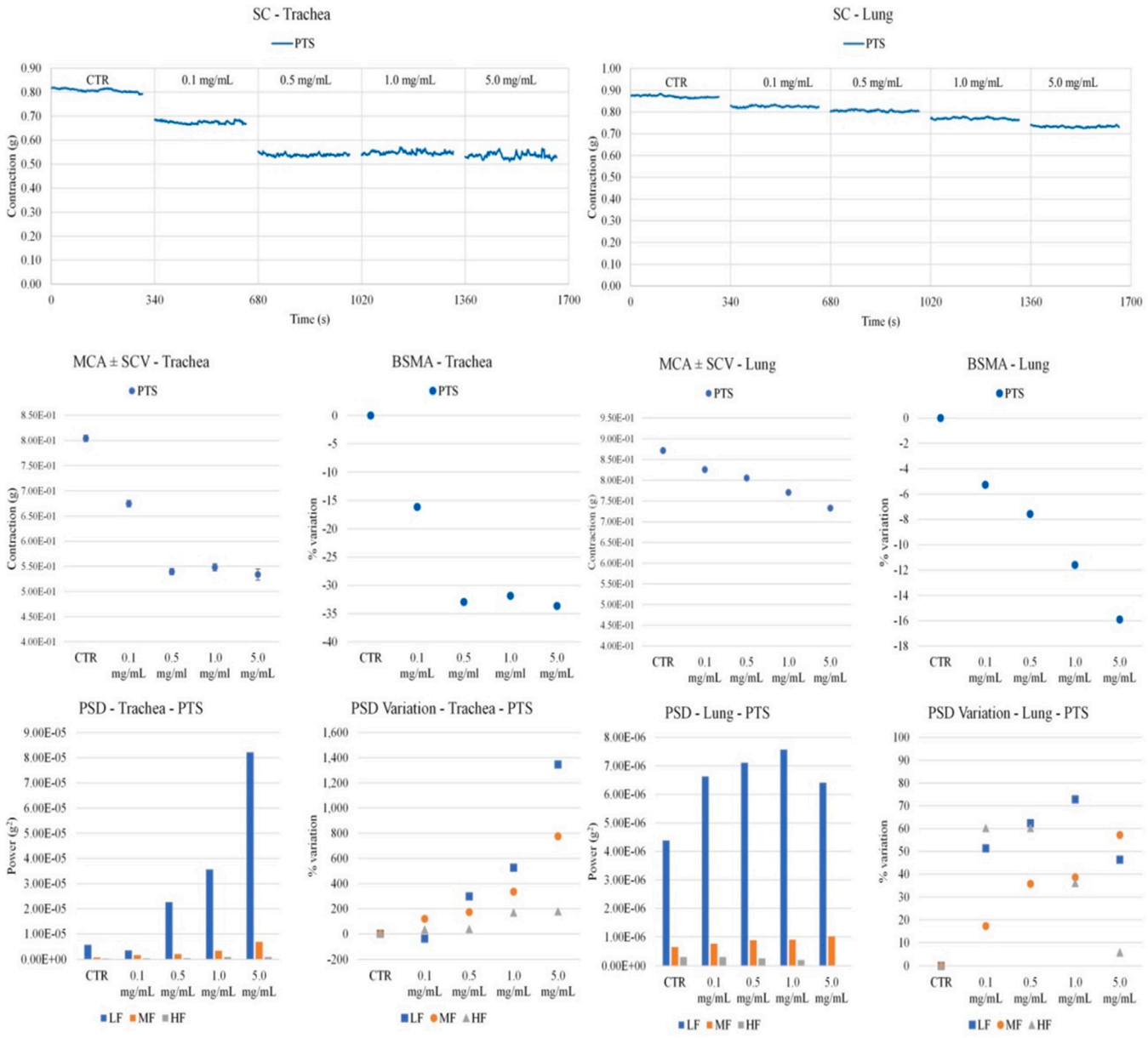

Fig. 5. The experimental original recording of the concentration-response curve of *P. tomentosa* extract (PTS), on spontaneous trachea and lung basal contractility. *Spontaneous Contraction (SC)-Trachea*: A) Signals for each concentration; B) Mean Contraction Amplitude (MCA) and Spontaneous Contraction Variability (SCV). All the comparisons are to be considered significant ($p < 0.05$). *SC-Lung*: D) Signals for each concentration; E) MCA and SCV. All the comparisons are to be considered significant ($p < 0.05$); C) and F) absolute powers (PSD) of the different bands of interest (LF: [0.0,0.2[Hz; MF: [0.2,0.6[Hz; HF: [0.6,1.0] Hz) and PSD% variations with respect to the control phase.

cannot be administered.

P. tomentosa extract derives from wood wastes. It was chemically characterized and its composition includes several compounds such as episesamin and sesamin. The study described here confirms that *P. tomentosa* extract exerts a virucidal effect from 0.1 to 0.005 mg/ml, a concentration range not detrimental to cell viability (Fig. 3B). Given the results of our assays, at the concentration of 0.1 mg/ml, *P. tomentosa* extract clearly shows a relevant antiviral effect too. There is a strong decrease in viral titers when the infected Vero E6 cells are treated with *P. tomentosa* extract, confirmed also by the presence of the viral genome by Real-Time RT-PCR (Fig. 3E).

The inhibition of the viral replication seems to be attributable, at least in part, to the inhibition of the main protease, called $3CL^{pro}$, involved in viral RNA transcription [45]. *P. tomentosa* extract inhibition of this enzyme is likely due to the presence of flavonoids [27]. In silico studies suggest that also sesamin may exert a role in this activity [46–48].

In the nutraceutical field, several substances act along with a different paradigm that we name *host* and *guest-oriented*, meaning the ability of these mixtures or isolated compounds to both hit viral targets and affect host functions involved in viral entry into host cells, and functions related to viral infection-induced detrimental effects, such as increased oxidative stress, inflammation, thrombosis and multiorgan failure.

The lung is the primary site of SARS-CoV-2-induced immunopathology, and blood vessels were presumed to be one of the main targets for the infection. Therefore, COVID-19 may be considered a vascular disease occurring mainly in the lungs.

SARS-CoV-2 binds to angiotensin-converting enzyme 2, decreasing the conversion of Angiotensin II to Angiotensin-[1–7] and favouring the

production of O_2^- and other radicals such as $OH^{\cdot}$ through the NADPH-oxidase, which increases along with the augment of neutrophils/lymphocytes ratio [49]. This increase in oxidative stress results in endothelium alterations and tissues damages. Furthermore, also S protein alone is able to damage endothelium cells as it enters mitochondria and inhibits endothelial nitric oxide (NO) synthase activity [50]. In this study, *P. tomentosa* extract was shown to inhibit viral replication interacting directly with $3CL^{pro}$ and S protein, potentially reducing also S protein-induced damages. Despite the lack of the dissociation constant determination due to the complexity of the sample, the interaction of *P. tomentosa* extract with the two proteins mentioned above is clearly visible and significant. Indeed, from the association phase (Fig. 4) it is possible to deduce the stoichiometry of the interaction, that probably involves more than a single compound since the sensorgram presents discontinuities that suggest the participation of fast interactions added to other slower ones, encouraging the study of the activity of each component of the sample with $3CL^{pro}$ and S protein.

In addition, *P. tomentosa* extract not only does not reduce lung epithelial cell viability at concentrations higher than those producing the antiviral effects (0.001–0.01 mg/ml), but it also exerts a protective action in those cells damaged by TBH, a toxic agent able to alter cell functions via increased oxidative stress. These data suggest a potential role of *P. tomentosa* extract in COVID-19 treatment, since its use in in vitro experimental models, can act both as an antiviral and a cytoprotective agent. The ability to abolish ROS production in H292 cells may be relevant in patients infected with SARS-CoV-2, decreasing the oxidative consequences of the viral infection. Moreover, airway smooth muscle contraction has a fundamental role in lung effective ventilation, and it is affected by some cytokines such as Interleukin 13 (IL-13) and Interleukin-17 [51] and it is related to inflammatory conditions. In fact, β2-agonist-induced response inhibition is associated with inflammatory conditions, characterized by an increase of inflammatory cytokines such as IL-13, Tumor Necrosis Factor (TNF)-α and Transforming Growth Factor (TGF)-β [52–54]. This event is due to, at least in part, the phosphorylation of $\beta-2$ adrenergic receptors triggered by G protein-coupled receptor kinase 2 and 3 that are upregulated in inflammatory conditions [55]. These phenomena partially explain the reduced functionality of smooth muscle of the trachea and lungs during inflammation. For this reason, we evaluated the effects of *P. tomentosa* extract on the trachea and lungs smooth muscle contractility, and we observed that this phyto complex exerts a relaxant effect in both tissues. These effects may be due to the presence of sesamin for its ability to affect the levels of NO and endothelin-1 [56] that influences respiratory smooth muscle contractility [57].

In addition, the maintenance of low-frequency oscillations and the reduction of tone that may result in a better flow of the gas, favouring exchange processes and producing a desirable effect in the treatment of respiratory tract infections, such as COVID-19, were observed. Furthermore, the *P. tomentosa* extract β-agonist action may be relevant in view of the use of the phyto complex in a respiratory medical device.

This extract may improve not only the oxidative stress and inflammatory status, but also the respiratory functions that undergo critical alterations in COVID-19 patients, in particular in those suffering from comorbidities, whose respiratory functions may be further worsened by opportunistic infections, such as mucormycosi [58].

5. Conclusion

This study originated with the goal of testing the biological activities of *P. tomentosa* extract. The results obtained from these tests are very promising. They confirm that *P. tomentosa* extract is an effective antiviral against SARS-CoV-2 and could involve directly the interaction with $3CL^{pro}$ and S protein. At the same time, they report cytoprotective, antioxidant and respiratory smooth muscle relaxant properties. The data suggest a potential role of *P. tomentosa* extract in COVID-19 treatment. However, this study has some limitations which we are aware of. Firstly, we focused on the treatment of cells after the infection of wild type of SARS-CoV-2 and not its major variants: we are planning to test *P. tomentosa* biological activities against Alpha, Beta, Delta and Omicron variants of SARS-CoV-2. Another limitation is the choice to use the Vero E6 cells only to assess virucidal and antiviral activities, although this model is commonly used to isolate, propagate and study SARS-CoV-like viruses and provide a suitable basis to perform antiviral compound screening [59].

In future studies, further experiments may be exerted in order to investigate the possibility to set up effective systems, such as nanotechnological systems, aimed at improving this vegetal extract's pharmacokinetic features [60,61]. Indeed, nanotechnology may exert a central role in the delivery of natural bioactive compounds and nutraceuticals in the management of COVID-19-related conditions.

In conclusion, this research confirms the relevant properties of *P. tomentosa* extract and paves the way for future studies in order to permit to confirm in vivo these significant results.

CRediT authorship contribution statement

Conceptualization: F. Magurano, M. Micucci, D. Nuzzo, M. D'Auria, ***Formal analysis and Investigati on:*** F. Magurano, M. Micucci, D. Nuzzo, P.Picone, M. Baggieri, S. Gioacchini, R. Fioravanti, P. Bucci, M. Kojouri, M. Mari, M. Retini, E. D'Ugo, A. Marchi, M. D'Auria, ***Data Curation and Writing - Original Draft***: F. Magurano, M. Micucci, D. Nuzzo, M. Baggieri, S. Gioacchini, R. Fioravanti, A. Marchi, M. D'Auria; V. Di Liberto; Roberta Budriesi, Laura Beatrice Mattioli, Ivan Corazza, Luigi Todaro, Marisabel Mecca, ***Writing - Review & Editing***: F. Magurano, D. Nuzzo, M. D'Auria, ***Approval of the version of the manuscript to be published:*** F. Magurano, M. Micucci, D. Nuzzo, M. Baggieri, P. Picone, S. Gioacchini, R. Fioravanti, P. Bucci, M. Kojouri, M. Mari, M. Retini, R. Budriesi, L. B. Mattioli, I. Corazza, V.Di Liberto, L. Todaro, E. D'Ugo, A. Marchi, M. Mecca, M. D'Auria, *Supervision*: F. Magurano, M. Micucci, D. Nuzzo, M. D'Auria.

Conflict of interest statement

The authors declare that they have no known competing financial interests or personal relationships that could have appeared to influence the work reported in this paper.

References

[1] S. Fiorino, F. Tateo, D. Biase, C.G. Gallo, P.E. Orlandi, I. Corazza, R. Budriesi, M. Micucci, M. Visani, E. Loggi, W. Hong, R. Pica, F. Lari, M. Zippi, SARS-CoV-2: lessons from both the history of medicine and from the biological behavior of other well-known viruses, Future Microbiol. 16 (14) (2021) 1105–1133, https://doi.org/10.2217/fmb-2021-0064.

[2] E. Lo Presti, D. Nuzzo, W. Al Mahmeed, K. Al-Rasadi, K. Al-Alawi, M. Banach, Y. Banerjee, A. Ceriello, M. Cesur, F. Cosentino, A. Firenze, M. Galia, S.Y. Goh, A. Janez, S. Kalra, N. Kapoor, P. Kempler, N. Lessan, P. Lotufo, N. Papanas, A. A. Rizvi, A. Sahebkar, R.D. Santos, A.P. Stoian, P.P. Toth, V. Viswanathan, M. Rizzo, CArdiometabolic Panel of International experts on Syndemic COvid-19 (CAPISCO). Molecular and pro-inflammatory aspects of COVID-19: the impact on cardiometabolic health, Biochim Biophys. Acta Mol. Basis Dis. 1868 (12) (2022 26), 166559, https://doi.org/10.1016/j.bbadis.2022.166559.

[3] P. Picone, T. Sanfilippo, R. Guggino, et al., Neurological consequences, mental health, physical care, and appropriate nutrition in long-COVID-19, Cell Mol. Neurobiol. (2022), https://doi.org/10.1007/s10571-022-01281-w.

[4] L. Urso, M.G. Distefano, G. Cambula, et al., The case of encephalitis in a COVID-19 pediatric patient, Neurol. Sci. 43 (2022) 105–112, https://doi.org/10.1007/s10072-021-05670-9.

[5] D. Nuzzo, S. Vasto, L. Scalisi, S. Cottone, G. Cambula, M. Rizzo, D. Giacomazza, P. Picone, Post-acute COVID-19 neurological syndrome: a new medical challenge, J. Clin. Med 10 (9) (2021 1) 1947, https://doi.org/10.3390/jcm10091947.

[6] D. Nuzzo, G. Cambula, I. Bacile, M. Rizzo, M. Galia, P. Mangiapane, P. Picone, D. Giacomazza, L. Scalisi, Long-term brain disorders in post Covid-19 neurological syndrome (PCNS) patient, Brain Sci. 11 (4) (2021 2) 454, https://doi.org/10.3390/brainsci11040454.

[7] M. Zippi, S. Fiorino, R. Budriesi, M. Micucci, I. Corazza, R. Pica, D. de Biase, C. G. Gallo, W. Hong, Paradoxical relationship between proton pump inhibitors and COVID-19: a systematic review and meta-analysis, World J. Clin. cases 9 (12) (2021) 2763–2777.

[8] W.H.O. Coronavirus (COVID-19) Dashboard. Available at: https://covid19.who.int/.

[9] M.S. Alam, D.M. Czajkowsky, SARS-CoV-2 infection and oxidative stress: pathophysiological insight into thrombosis and therapeutic opportunities, Cytokine Growth Factor Rev. 63 (2022) 44–57, https://doi.org/10.1016/j.cytogfr.2021.11.001.

[10] M. Ionescu, A.P. Stoian, M. Rizzo, D. Serban, D. Nuzzo, L. Mazilu, A.I. Suceveanu, A.M. Dascalu, I.R. Parepa, The role of endothelium in COVID-19, Int J. Mol. Sci. 22 (21) (2021 3) 11920, https://doi.org/10.3390/ijms222111920.

[11] World Health Organization, WHO Global Report on Traditional and Complementary Medicine 2019, World Health Organization, 2019. https://apps.who.int/iris/handle/10665/312342.

[12] M.M. Rahman, M.R. Islam, S. Shohag, M.E. Hossain, M. Shah, S.K. Shuvo, H. Khan, M.A.R. Chowdhury, I.J. Bulbul, M.S. Hossain, S. Sultana, M. Ahmed, M.F. Akhtar, A. Saleem, M.H. Rahman, Multifaceted role of natural sources for COVID-19 pandemic as marine drugs, Environ. Sci. Pollut. Res Int 29 (31) (2022) 46527–46550, https://doi.org/10.1007/s11356-022-20328-5.

[13] F. Islam, S. Bibi, A.F.K. Meem, M.M. Islam, M.S. Rahaman, S. Bepary, M. M. Rahman, M.M. Rahman, A. Elzaki, S. Kajoak, H. Osman, M. ElSamani, M. U. Khandaker, A.M. Idris, T.B. Emran, Natural bioactive molecules: an alternative approach to the treatment and control of COVID-19, Int J. Mol. Sci. 22 (23) (2021) 12638, https://doi.org/10.3390/ijms222312638.

[14] M.M. Rahman, M.R. Islam, S. Akash, S.A. Mim, M.S. Rahaman, T.B. Emran, E. K. Akkol, R. Sharma, F.A. Alhumaydhi, S.H. Sweilam, M.E. Hossain, T.K. Ray, S. Sultana, M. Ahmed, E. Sobarzo-Sánchez, P. Wilairatana, In silico investigation and potential therapeutic approaches of natural products for COVID-19: Computer-aided drug design perspective, Front Cell Infect. Microbiol 12 (2022), 929430, https://doi.org/10.3389/fcimb.2022.929430.

[15] F. Magurano, M. Sucameli, P. Picone, M. Micucci, M. Baggieri, A. Marchi, P. Bucci, S. Gioacchini, G. Catinella, G. Borgonovo, S. Dallavalle, D. Nuzzo, A. Pinto, Antioxidant activity of citrus limonoids and investigation of their virucidal potential against SARS-CoV-2 in cellular models, Antioxidants 10 (11) (2021) 1794, https://doi.org/10.3390/antiox10111794.

[16] G. Annunziata, M. Sanduzzi Zamparelli, C. Santoro, R. Ciampaglia, M. Stornaiuolo, G.C. Tenore, A. Sanduzzi, E. Novellino, May polyphenols have a role against coronavirus infection? An overview of in vitro evidence, Front. Med. 7 (2020) 240, https://doi.org/10.3389/fmed.2020.00240.

[17] M.H. Farzaei, A.K. Singh, R. Kumar, C.R. Croley, A.K. Pandey, E. Coy-Barrera, J. Kumar Patra, G. Das, R.G. Kerry, G. Annunziata, G.C. Tenore, H. Khan, M. Micucci, R. Budriesi, S. Momtaz, S.M. Nabavi, A. Bishayee, Targeting inflammation by flavonoids: novel therapeutic strategy for metabolic disorders, Int. J. Mol. Sci. 20 (19) (2019) 4957, https://doi.org/10.3390/ijms20194957.

[18] K. Zeka, K. Ruparelia, R. Arroo, R. Budriesi, M. Micucci, Flavonoids and their metabolites: prevention in cardiovascular diseases and diabetes, Dis. (Basel, Switz.) 5 (3) (2017) 19, https://doi.org/10.3390/diseases5030019.

[19] M. Bahun, M. Jukić, D. Oblak, L. Kranjc, G. Bajc, M. Butala, K. Bozovičar, T. Bratkovič, Č. Podlipnik, N. Poklar Ulrih, Inhibition of the SARS-CoV-2 3CLpro main protease by plant polyphenols, Food Chem. 373 (Pt B) (2022), 131594, https://doi.org/10.1016/j.foodchem.2021.13159.

[20] S. Sanduzzi Zamparelli, L. Capitelli, N. Coppola, C. Venditto, C. Santoro, G. Annunziata, D. Bruzzese, N. Cuomo, I. Gentile, M. Bocchino, A. Sanduzzi Zamparelli, A phase ii study on the effect of taurisolo® administered via AEROsol in hospitalized patients with mild to moderate COVID-19 pneumonia: the TAEROVID-19 study, Cells 11 (9) (2022) 1499, https://doi.org/10.3390/cells11091499.

[21] J. Choe, P. Har Yong, Z. Xiang Ng, The efficacy of traditional medicinal plants in modulating the main protease of SARS-CoV-2 and cytokine storm, Chem. Biodivers. (2022 20), e202200655, https://doi.org/10.1002/cbdv.202200655.

[22] M.M. Rahman, S. Shohag, M.R. Islam, S. Akhter, S.A. Mim, R. Sharma, A. Rauf, An insight into COVID-19 and traditional herbs: bangladesh perspective, Med Chem. (2022 29), https://doi.org/10.2174/1573406418666220829144746.

[23] G. Annunziata, M. Maisto, C. Schisano, R. Ciampaglia, V. Narciso, G.C. Tenore, E. Novellino, Effects of grape pomace polyphenolic extract (Taurisolo®) in reducing TMAO serum levels in humans: preliminary results from a randomized, placebo-controlled, cross-over study, Nutrients 11 (1) (2019) 139, https://doi.org/10.3390/nu11010139.

[24] L. Diniz, C. Bezerra Filho, B.C. Fielding, D.P. de Sousa, Natural antioxidants: a review of studies on human and animal coronavirus, Oxid. Med. Cell. Longev. 2020 (2020) 3173281, https://doi.org/10.1155/2020/3173281.

[25] M. D'Auria, M. Mecca, L. Todaro, High temperature treatment allows the detection of episesamin in paulownia wood extractives, Nat. Prod. Res. 34 (9) (2020) 1326–1330, https://doi.org/10.1080/14786419.2018.1560289.

[26] K. Smejkal, P. Holubova, A. Zima, J. Muselik, M. Dvorska, Antiradical activity of Paulownia tomentosa (Scrophulariaceae) extracts, Molecules 12 (6) (2007) 1210–1219, https://doi.org/10.3390/12061210.

[27] J.K. Cho, M.J. Curtis-Long, K.H. Lee, D.W. Kim, H.W. Ryu, H.J. Yuk, K.H. Park, Geranylated flavonoids displaying SARS-CoV papain-like protease inhibition from the fruits of Paulownia tomentosa, Bioorg. Med. Chem. 21 (11) (2013) 3051–3057, https://doi.org/10.1016/j.bmc.2013.03.027.

[28] M. Mecca, L. Todaro, M. D'Auria, The use of a molybdenum polyoxometalated compound to increase the amount of extractives from wood wastes, Biomolecules 8 (3) (2018) 62, https://doi.org/10.3390/biom8030062.

[29] S. Ferrari, I. Cuccui, O. Allegretti, Thermo-vacuum modification of some european softwood and hardwood species treated at different conditions, BioResources 8 (2013) 1100–1109.

[30] O. Allegretti, M. Brunetti, I. Cuccui, S. Ferrari, M. Nocetti, N. Terziev, Thermo-vacuum modification of spruce (Picea abies karst.) and fir (Abies alba mill.) wood, BioResources 7 (2012) 3656–3669.

[31] TAPPI, Solvent extractives of wood and pulp. TAPPI Test Method T204, TMCD-04, technical association of the pulp and paper industry, Atlanta, GA, USA (2004) 1–12.

[32] D. Nuzzo, M. Scordino, A. Scurria, C. Giardina, F. Giordano, F. Meneguzzo, G. Mudò, M. Pagliaro, P. Picone, A. Attanzio, S. Raimondo, R. Ciriminna, V. Di Liberto, Protective, antioxidant and antiproliferative activity of grapefruit integropectin on SH-SY5Y cells, Int. J. Mol. Sci. 22 (17) (2021) 9368, https://doi.org/10.3390/ijms22179368.

[33] F. Magurano, M. Baggieri, A. Marchi, G. Rezza, L. Nicoletti, COVID-19 Study Group, SARS-CoV-2 infection: the environmental endurance of the virus can be influenced by the increase in temperature, Clin. Microbiol. Infect. Feb;27 (2) (2021) 289.e5–289.e7, https://doi.org/10.1016/j.cmi.2020.10.034.

[34] CDC 2020. 2019-Novel Coronavirus (2019-nCoV) Real-time rRT-PCR Panel Primers and Probes. Updated: May 29, 2020.

[35] G.A. Papalia, S. Leavitt, M.A. Bynum, P.S. Katsamba, R. Wilton, H. Qiu, M. Steukers, S. Wang, L. Bindu, S. Phogat, A.M. Giannetti, T.E. Ryan, V.A. Pudlak, K. Matusiewicz, K.M. Michelson, A. Nowakowski, A. Pham-Baginski, J. Brooks, B. C. Tieman, B.D. Bruce, M. Vaughn, M. Baksh, Y.H. Cho, M.D. Wit, A. Smets, J. Vandersmissen, L. Michiels, D.G. Myszka, Comparative analysis of 10 small molecules binding to carbonic anhydrase II by different investigators using Biacore technology, Anal. Biochem. 359 (1) (2006) 94–105, https://doi.org/10.1016/j.ab.2006.08.021.

[36] B. Chen, SPR biosensor as a tool for screening prion protein binders as potential anti prion leads, Methods Mol. Biol. 627 (2010) 147–155, https://doi.org/10.1007/978-1-60761-670-2_9.

[37] R. Budriesi, P. Ioan, A. Leoni, N. Pedemonte, A. Locatelli, M. Micucci, A. Chiarini, L.J.V. Galietta, Cystic fibrosis: a new target for 4-imidazo[2,1-b]thiazole-1,4-dihydropyridines, J. Med. Chem. 54 (2011) 3885–3894, https://doi.org/10.1021/jm200199r.

[38] M. Micucci, M. Malaguti, T.G. Toschi, G. Di Lecce, R. Aldini, A. Angeletti, A. Chiarini, R. Budriesi, S. Hrelia, Cardiac and vascular synergic protective effect of olea europea L. leaves and hibiscus sabdariffa L. flower extracts, Oxid. Med. Cell. Longev. (2015), 318125, https://doi.org/10.1155/2015/318125.

[39] L.B. Mattioli, M. Frosini, R. Amoroso, C. Maccallini, E. Chiano, R. Aldini, F. Urso, I. Corazza, M. Micucci, R. Budriesi, Olea europea L. Leaves and Hibiscus sabdariffa L. petals extracts: herbal mix from cardiovascular network target to gut motility dysfunction application, Nutrients 14 (2022) 463, https://doi.org/10.3390/nu14030463.

[40] M. Micucci, M. Protti, R. Aldini, M. Frosini, I. Corazza, C. Marzetti, L.B. Mattioli, G. Tocci, A. Chiarini, L. Mercolini, R. Brudriesi, Thymus vulgaris L. essential oil solid formulation: chemical profile, spasmolytic and antimicrobial effects, Biomolecules 10 (2020) 860, https://doi.org/10.3390/biom10060860.

[41] Tallarida R.J., Murray R.B. (1987) Manual of Pharmacologic Calculations with Computer Programs, version 4.2, Springer-Verlag: New York.

[42] Motulsky H., Christopoulos A. (2003) Fitting models to biological data using linear and non linear regression, a practical guide to curve fitting. GraphPad Software Inc., San Diego CA, Available online: chrome-extension://efaidnbmnnnibpcajpcglclefindmkaj/https://www.facm.ucl.ac.be/cooperation/Vietnam/WBI-Vietnam-October-2011/Modelling/RegressionBook.pdf (Accessed 7 June 2021).

[43] Motulsky, H.J. (2007) Prism 5 Statistics Guide. GraphPad Software Inc., San Diego CA, USA; Available online: chrome-extension://efaidnbmnnnibpcajpcglclefindmkaj/https://cdn.graphpad.com/faq/2/file/Prism_v5_Statistics_Guide.pdf.

[44] D. Nuzzo, G. Presti, P. Picone, G. Galizzi, E. Gulotta, S. Giuliano, C. Mannino, V. Gambino, S. Scoglio, M. Di Carlo, Effects of the aphanizomenon flos-aquae extract (Klamin®) on a neurodegeneration cellular model, Oxid. Med Cell Longev. 2018 (2018 17) 9089016, https://doi.org/10.1155/2018/9089016.

[45] Z. Jin, Y. Zhao, Y. Sun, B. Zhang, H. Wang, Y. Wu, Y. Zhu, C. Zhu, T. Hu, X. Du, Y. Duan, J. Yu, X. Yang, X. Yang, K. Yang, X. Liu, L.W. Guddat, G. Xiao, L. Zhang, H. Yang, Z. Rao, Structural basis for the inhibition of SARS-CoV-2 main protease by antineoplastic drug carmofur, Nat. Struct. Mol. Biol. 27 (6) (2020) 529–532, https://doi.org/10.1038/s41594-020-0440-6.

[46] A. Kumar, D.C. Mishra, U.B. Angadi, R. Yadav, A. Rai, D. Kumar, Inhibition potencies of phytochemicals derived from sesame against SARS-CoV-2 main protease: a molecular docking and simulation study, Front. Chem. 9 (2021), 744376, https://doi.org/10.3389/fchem.2021.744376.

[47] A.K. Pandey, S. Verma, An in-silico evaluation of dietary components for structural inhibition of SARS-CoV-2 main protease, J. Biomol. Struct. Dyn. 40 (1) (2022) 136–142, https://doi.org/10.1080/07391102.2020.1809522.

[48] A.K. Umar, J.H. Zothantluanga, K. Aswin, S. Maulana, M. Sulaiman Zubair, H. Lalhlenmawia, M. Rudrapal, D. Chetia, Antiviral phytocompounds "ellagic acid" and "(+)-sesamin" of Bridelia retusa identified as potential inhibitors of SARS-CoV-2 3CL pro using extensive molecular docking, molecular dynamics simulation studies, binding free energy calculations, and bioactivity prediction, Struct. Chem. 33 (5) (2022) 1445–1465, https://doi.org/10.1007/s11224-022-01959-3.

[49] G. El-Arif, S. Khazaal, A. Farhat, J. Harb, C. Annweiler, Y. Wu, Z. Cao, H. Kovacic, Z. Abi Khattar, Z. Fajloun, J.M. Sabatier, Angiotensin II type i receptor (AT1R): the gate towards COVID-19-Associated diseases, Molecules 27 (7) (2022) 2048, https://doi.org/10.3390/molecules27072048.

[50] S. Lei, F. Jiang, W. Su, C. Chen, J. Chen, W. Mei, L.Y. Zhan, Y. Jia, L. Zhang, D. Liu, Z.Y. Xia, Z. Xia, Clinical characteristics and outcomes of patients undergoing surgeries during the incubation period of COVID-19 infection, EClinicalMedicine 21 (2020), 100331, https://doi.org/10.1016/j.eclinm.2020.100331.

[51] Y.H. Zhang, Z. Li, T. Zeng, L. Chen, H. Li, T. Huang, Y.D. Cai, Detecting the multiomics signatures of factor-specific inflammatory effects on airway smooth muscles, Front. Genet. 11 (2021), 599970, https://doi.org/10.3389/fgene.2020.599970.

[52] C.A. Ojiaku, E. Chung, V. Parikh, J.K. Williams, A. Schwab, A.L. Fuentes, M. L. Corpuz, V. Lui, S. Paek, N.M. Bexiga, S. Narayan, F.J. Nunez, K. Ahn, R. S. Ostrom, S.S. An, R.A. Panettieri Jr, Transforming growth factor-β1 decreases β2-agonist-induced relaxation in human airway smooth muscle, Am. J. Respir. Cell Mol. Biol. 61 (2) (2019) 209–218.

[53] C.J. Koziol-White, E.J. Yoo, G. Cao, J. Zhang, E. Papanikolaou, I. Pushkarsky, A. Andrews, B.E. Himes, R.D. Damoiseaux, S.B. Liggett, D. Di Carlo, R.C. Kurten, R. A. Panettieri Jr, Inhibition of PI3K promotes dilation of human small airways in a rho kinase-dependent manner, Br. J. Pharmacol. 173 (18) (2016) 2726–2738, https://doi.org/10.1111/bph.13542.

[54] K. Hotta, C.W. Emala, C.A. Hirshman, TNF-alpha upregulates Gialpha and Gqalpha protein expression and function in human airway smooth muscle cells, Am. J. Physiol. 276 (3) (1999) L405–L411.

[55] L. Chachi, A. Alzahrani, C. Koziol-White, M. Biddle, R. Bagadood, R. A. Panettieri Jr, P. Bradding, Y. Amrani, Increased β2-adrenoceptor phosphorylation in airway smooth muscle in severe asthma: possible role of mast cell-derived growth factors, Clin. Exp. Immunol. 194 (2) (2018) 253–258, https://doi.org/10.1111/cei.13191.

[56] C.C. Lee, P.R. Chen, S. Lin, S.C. Tsai, B.W. Wang, W.W. Chen, C.E. Tsai, K.G. Shyu, Sesamin induces nitric oxide and decreases endothelium–1 production in HUVECs: possible implications for its antihypertensive effect, J. Hypertens. 22 (2004) 2329–2338, https://doi.org/10.1097/00004872-200412000-00015.

[57] S.R. O'Donnell, J.C. Wanstall, X.P. Zeng, Pinacidil antagonism of endothelin-induced contractions of smooth muscle in the lungs: differences between tracheal and pulmonary artery preparations, J. Pharm. Exp. Ther. 252 (3) (1990) 1318–1323.

[58] M.R. Islam, M.M. Rahman, M.T. Ahasan, N. Sarkar, S. Akash, M. Islam, F. Islam, M. N. Aktar, M. Saeed, M. Harun-Or-Rashid, M.K. Hosain, M.S. Rahaman, S. Afroz, S. Bibi, M.H. Rahman, S.H. Sweilam, The impact of mucormycosis (black fungus) on SARS-CoV-2-infected patients: at a glance, Environ. Sci. Pollut. Res Int 29 (46) (2022) 69341–69366, https://doi.org/10.1007/s11356-022-22204-8.

[59] N.S. Ogando, T.J. Dalebout, J.C. Zevenhoven-Dobbe, R.W.A.L. Limpens, Y. van der Meer, L. Caly, J. Druce, J.J.C. de Vries, M. Kikkert, M. Bárcena, I. Sidorov, E. J. Snijder, SARS-coronavirus-2 replication in Vero E6 cells: replication kinetics, rapid adaptation and cytopathology, J. Gen. Virol. 101 (9) (2020) 925–940, https://doi.org/10.1099/jgv.0.001453.

[60] M.M. Rahman, M. Ahmed, M.T. Islam, M.R. Khan, S. Sultana, S.K. Maeesa, S. Hasan, M.A. Hossain, K.S. Ferdous, B. Mathew, A. Rauf, M.S. Uddin, Nanotechnology-based approaches and investigational therapeutics against COVID-19, Curr. Pharm. Des. 28 (12) (2022) 948–968, https://doi.org/10.2174/1381612827666210701150315.

[61] A. Rauf, T. Abu-Izneid, A.A. Khalil, N. Hafeez, A. Olatunde, M. Rahman, P. Semwal, Y.S. Al-Awthan, O.S. Bahattab, I.N. Khan, M.A. Khan, R. Sharma, Nanoparticles in clinical trials of COVID-19: an update, Int J. Surg. 104 (2022), 106818.